Delbrück scattering calculations

Paul Papatzacos and Kjell Mork
Institute of Physics, University of Trondheim, Norges Laererhøgskole, Trondheim. Norway
(Received 12 March 1975)

The cross section for elastic scattering of photons on a static Coulomb potential, Delbrück scattering, is calculated in the lowest-order Born approximation. Using conventional Feynman techniques and gauge invariance we obtain expressions for the real and imaginary parts of the scattering amplitude for polarized photons. These rather complicated expressions contain multidimensional integrals which have been evaluated partly by analytical and partly by numerical methods, and Delbrück amplitudes have been obtained for various scattering angles and for photon energies ω varying from zero to several GeV. The results confirm earlier calculations at very low energies ($\omega \ll 1$ MeV), confirm the imaginary parts but disagree with the real parts previously obtained by Ehlotzky and Sheppey for $\omega < 20$ MeV, and confirm the high-energy results of Cheng and Wu to lowest order. A comparison with some recent experiments is shown.

I. INTRODUCTION

Delbrück scattering is the reaction in which photons scatter elastically in a static Coulomb potential. The process is impossible in linear electromagnetism, but as was first pointed out by Delbrück[1] in 1933, it is possible in relativistic quantum theory because of vacuum polarization. This relation to nonlinearity and vacuum polarization has inspired many authors to work on the process. We shall not mention all of them here,[2] but important contributions have been made by Karplus and Neuman,[3] Rohrlich and Glückstern,[4] Kessler,[5] Zernik,[6] Ehlotzky and Sheppey,[7] Costantini *et al.*,[8] and Cheng and Wu.[9] The Delbrück amplitude is, however, rather complex and difficult to calculate, so Delbrück cross sections of experimental interest were known only for energies below 20 MeV (cf. Refs. 5, 6, and 7) and for very high energies (cf. Ref. 9). The motivation for the present work was therefore primarily to find the cross section for a wider range of energies, but we also considered it useful to provide a check of previous results by an independent method.

In Sec. II we construct the Delbrück amplitude using the usual Feynman techniques. Gauge invariance is applied to write the amplitude in a convenient form, and we show how the sevenfold integrals involved can be reduced to fourfold ones by analytic integrations. The remaining integrals are integrated numerically.

In Sec. III we present the results. Values for the real and imaginary parts of the linear polarization amplitudes are given for some photon energies and scattering angles. Finally in Sec. IV the results are compared with experimental numbers.

We use units in which $\hbar = c = 1$, and for a particle with momentum $\vec{k}$ and energy ω we define the four-vector $k = (\vec{k}, k_4)$ with $k_4 = i\omega$.

II. CALCULATION OF THE DELBRÜCK AMPLITUDE

A. Gauge-invariant expression for the amplitude

To lowest order in the electron charge e the Delbrück amplitude is described by the box diagrams in Fig. 1, and it is of order $e^6 Z^2$, where Z is the atomic number (note that diagrams with three corners do not contribute according to Furry's theorem). Using the Feynman rules we may write the cross section in the form

$$\frac{d\sigma}{d\Omega} = |A|^2 = (\alpha Z)^4 r_0^2 |a|^2 , \tag{1}$$

where $\alpha \simeq \frac{1}{137}$ is the fine-structure constant, r_0 is the classical radius of the electron, and the amplitude a is

$$a = -ie_i e_j' P_{ij} . \tag{2}$$

Here e_i and e_j' are the polarization vectors, for linear polarization, of the incoming photon with four-vector k and the outgoing photon with four-vector k', respectively. The tensor P_{ij} is

$$P_{ij} = \frac{m}{8\pi^5} \int \frac{d^3q}{\vec{q}^{\,2}} \frac{1}{(\vec{q} - \vec{\Delta})^2} \Pi_{ij44}(k, k', q) , \tag{3}$$

where $\vec{\Delta}$ is the momentum transfer

$$\vec{\Delta} = \vec{k} - \vec{k}' , \tag{4}$$

and Π_{ij44} are components of the fourth-order

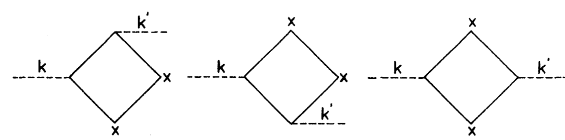

FIG. 1. Delbrück diagrams. The interaction with a Coulomb field is indicated by an ×. The incoming and outgoing photons are marked by k and k', respectively.

vacuum-polarization tensor $\Pi_{\mu\nu\lambda\sigma}(k,k',q)$ with $q_4=0$ and $\omega=\omega'$. This tensor is

$$\Pi_{\mu\nu\lambda\sigma}(k,k',q)=G_{\mu\nu\lambda\sigma}(k,k',q)-G_{\mu\nu\lambda\sigma}(0,0,0)\,, \tag{5}$$

where

$$G_{\mu\nu\lambda\sigma}(k,k',q)=T_{\mu\nu\lambda\sigma}(k,k',q)+T_{\nu\mu\lambda\sigma}(-k',-k,q)+T_{\mu\lambda\nu\sigma}(k,q,k') \tag{6}$$

and

$$T_{\mu\nu\lambda\sigma}(k,k',q)=\int d^4p\,\mathrm{Tr}\left(\gamma_\mu\frac{1}{i\gamma\cdot p+m}\gamma_\nu\frac{1}{i\gamma\cdot(p-k')+m}\gamma_\lambda\frac{1}{i\gamma\cdot(p-k'-q)+m}\gamma_\sigma\frac{1}{i\gamma\cdot(p-k)+m}\right). \tag{7}$$

The tensor $G_{\mu\nu\lambda\sigma}$ in Eq. (5) contains three terms which, respectively, give the contributions from the diagrams in Fig. 1 in a straightforward way. As is easily seen from (7) each term diverges logarithmically for large p, but, as is well known, the divergences cancel in $G_{\mu\nu\lambda\sigma}$. However, convergence does not guarantee correctness, and one may easily show that $G_{\mu\nu\lambda\sigma}$ is not gauge-invariant. The correct, gauge-invariant, vacuum-polarization tensor $\Pi_{\mu\nu\lambda\sigma}$ is obtained in Eq. (5) by a subtraction procedure. Various arguments lead to this procedure[3,10]; some details are given in Ref. 11.

The general tensor $\Pi_{\mu\nu\lambda\sigma}$ is in Eq. (3) specialized to the case of Delbrück scattering, with two Coulomb field interactions and no energy transfer.

The form (5) of $\Pi_{\mu\nu\lambda\sigma}$ is, however, not very convenient for our purpose. Cancellations are usually harmful to the accuracy in numerical calculations, and we therefore adopt another method which was first employed by Karplus and Neuman[3,12] for photon-photon scattering, and later by Shima[13] for photon-splitting calculations, and also by Costantini *et al.*[8]

We introduce the notation

$$k^{(1)}=k\,,\quad k^{(2)}=k'\,,\quad k^{(3)}=q\,,\ \text{with } k_4^{(3)}=0\,. \tag{8}$$

The corresponding polarization vectors $e^{(i)}$ satisfy $e^{(i)}\cdot k^{(i)}=0$ and $e_4^{(i)}=0$ for $i=1$ and 2. Since $\Pi_{\mu\nu\sigma\lambda}$ is a tensor depending on k, k', and q, it can be written in the form

$$\begin{aligned}\Pi_{\mu\nu\lambda\sigma}(k^{(1)},k^{(2)},k^{(3)})=&\sum_{i,j,l,m=1}^{3}A^{ijlm}k_\mu^{(i)}k_\nu^{(j)}k_\lambda^{(l)}k_\sigma^{(m)}\\&+\sum_{i,j=1}^{3}(B_1^{ij}\delta_{\mu\nu}k_\lambda^{(i)}k_\sigma^{(j)}+B_2^{ij}\delta_{\mu\lambda}k_\nu^{(i)}k_\sigma^{(j)}\\&\quad+B_3^{ij}\delta_{\mu\sigma}k_\nu^{(i)}k_\lambda^{(j)}+B_4^{ij}\delta_{\nu\lambda}k_\mu^{(i)}k_\sigma^{(j)}+B_5^{ij}\delta_{\nu\sigma}k_\mu^{(i)}k_\lambda^{(j)}+B_6^{ij}\delta_{\lambda\sigma}k_\mu^{(i)}k_\nu^{(j)})\\&+C_1\delta_{\mu\nu}\delta_{\lambda\sigma}+C_2\delta_{\mu\lambda}\delta_{\nu\sigma}+C_3\delta_{\mu\sigma}\delta_{\nu\lambda}\,,\end{aligned} \tag{9}$$

where A, B, and C are functions of invariant products $k^{(i)}\cdot k^{(j)}$. Gauge invariance implies

$$k_\mu^{(1)}\Pi_{\mu\nu\lambda\sigma}=k_\nu^{(2)}\Pi_{\mu\nu\lambda\sigma}=k_\lambda^{(3)}\Pi_{\mu\nu\lambda\sigma}=0\,, \tag{10}$$

and these identities can be used to express all B and C coefficients in (9) in terms of the A's. The important advantage of this method is that the A coefficients come from the most convergent terms in the p integration in (7), and they are not influenced by the subtraction of $G_{\mu\nu\lambda\sigma}(0,0,0)$ in (5).

For Delbrück scattering we need

$$\begin{aligned}e_\mu^{(1)}e_\nu^{(2)}\Pi_{\mu\nu44}=&\sum_{i=2,3;\,j=1,3;\,l,m=1,2}A^{ijlm}(e^{(1)}k^{(i)})(e^{(2)}k^{(j)})k_4^{(l)}k_4^{(m)}+\sum_{l,m=1,2}B_1^{lm}(e^{(1)}e^{(2)})k_4^{(l)}k_4^{(m)}\\&+\sum_{i=2,3;\,j=1,3}B_6^{ij}(e^{(1)}k^{(i)})(e^{(2)}k^{(j)})+C_1(e^{(1)}e^{(2)})\,,\end{aligned} \tag{11}$$

and we therefore must express the coefficients B_1^{11}, B_1^{12}, B_1^{21}, B_1^{22}, B_6^{21}, B_6^{23}, B_6^{31}, B_6^{33}, and C_1 in terms of the so-called leading coefficients A^{ijkl}. This calculation is shown in Appendix A. The result is

$$\begin{aligned} e_\mu e'_\nu \Pi_{\mu\nu 44} = ee'\{&\omega^2 kk' S_{21} + q^2[kqA^{3133} + kk'A^{2133} - \omega^2(A^{3132} + A^{2331})] + kq[kk'A^{2113} + \omega^2 S_2 + k'qS_1] + k'q[kk'A^{2123} - \omega^2 S_2]\} \\ &- (ek')(e'k)[\omega^2 S_{21} + q^2 A^{2133} + kqA^{2113} + k'qA^{2123}] - (ek')(e'q)[\omega^2 S_{23} + q^2 A^{2333} + kqS_1] \\ &- (e'k)(eq)[\omega^2 S_{31} + q^2 A^{3133} + k'qS_1] - (eq)(e'q)[\omega^2 S_{32} + q^2 A^{3333} - kk'S_1], \end{aligned} \tag{12}$$

with

$$S_{ij} = \sum_{k,l=1}^{2} A^{ijkl}, \quad S_1 = A^{2313} + A^{3123}, \quad S_2 = A^{3122} - A^{2311}. \tag{13}$$

Note that relations between the A's, which may be derived from crossing symmetry (cf. Refs. 3 and 8), are not useful for our numerical calculations. The number of different A's appearing in (12) is 26 and we shall show how to compute these quantities.

Since the coefficients A which are defined by Eq. (9) are not affected by the subtraction of $G_{\mu\nu\lambda\sigma}(0,0,0)$ in (5), they may be calculated directly from the tensor $G_{\mu\nu\lambda\sigma}$ given by (6). This equation may be written as

$$G_{\mu\nu\lambda\sigma}(k,k',q) = \sum_{i=1}^{3} T^{(i)}_{\mu\nu\lambda\sigma}(k,k',q), \tag{14}$$

with

$$\begin{aligned} T^{(1)}_{\mu\nu\lambda\sigma}(k,k',q) &= T_{\mu\nu\lambda\sigma}(k,k',q), \\ T^{(2)}_{\mu\nu\lambda\sigma}(k,k',q) &= T^{(1)}_{\nu\mu\lambda\sigma}(-k',-k,q), \\ T^{(3)}_{\mu\nu\lambda\sigma}(k,k',q) &= T^{(1)}_{\mu\lambda\nu\sigma}(k,q,k'). \end{aligned} \tag{15}$$

Now each tensor $T^{(i)}_{\mu\nu\lambda\sigma}$ can be written in a form similar to (9), and consequently we have

$$A^{ijlm} = \sum_{n=1}^{3} A_n^{ijlm}, \tag{16}$$

where now the A_n^{ijlm} pertain to $T^{(n)}_{\mu\nu\lambda\sigma}$.

It remains to calculate the A_n^{ijlm} for $n=1$, 2, and 3. Actually the case $n=2$ need not be considered separately, as we shall see later. The 26 values of $ijlm$ appearing in (12) are 2111, 2112, 2113, 2121, 2122, 2123, 2133, 2311, 2312, 2313, 2321, 2322, 2331, 2333, 3111, 3112, 3121, 3122, 3123, 3132, 3133, 3311, 3312, 3321, 3322, and 3333, respectively.

B. The integration over the loop momentum p

The tensor $T^{(1)}_{\mu\nu\lambda\sigma}$ is given by Eq. (7). In order to integrate over d^4p we introduce three Feynman parameters x, y, and z, and thus

$$T^{(1)}_{\mu\nu\lambda\sigma} = 6\int_0^1 dx \int_0^x dy \int_0^y dz \int d^4p \frac{N_1}{[(p-P_1)^2 + D_1]^4}, \tag{17}$$

where

$$\begin{aligned} N_1 = \mathrm{Tr}\{&\gamma_\mu(i\gamma\cdot p - m)\gamma_\nu[i\gamma\cdot(p-k') - m]\gamma_\lambda \\ &\times[i\gamma\cdot(p-k'-q) - m]\gamma_\sigma[i\gamma\cdot(p-k) - m]\}, \end{aligned} \tag{18}$$

$$P_1 = l_1^{(1)}k + l_2^{(1)}k' + l_3^{(1)}q, \tag{19}$$

$$D_1 = \lambda_1(\vec{q}^2 - 2\vec{q}\cdot\vec{Q} + \omega^2\mu_1), \quad \vec{Q} = \kappa_1\vec{k} - \kappa'_1\vec{k}', \tag{20}$$

and $l_i^{(1)}$, λ_1, κ_1, κ'_1, and μ_1 are dimensionless functions of x, y, and z; μ_1 depends in addition on ω/m and the scattering angle θ. Explicit expressions are given in Appendix B 1.

Now, changing to a new variable $p' = p - P_1$ in (17) we obtain the simple denominator $(p'^2 + D_1)^4$, and it is easily seen that the only term in N_1 which contributes to the A's is

$$\begin{aligned} N_1^A &= \mathrm{Tr}\{\gamma_\mu(\gamma\cdot P_1)\gamma_\nu\gamma\cdot(P_1 - k')\gamma_\lambda\gamma \\ &\quad\cdot(P_1 - k' - q)\gamma_\sigma\gamma\cdot(P_1 - k)\} \\ &= \mathrm{Tr}\{\gamma_\mu\gamma_\alpha\gamma_\nu\gamma_\beta\gamma_\lambda\gamma_\gamma\gamma_\sigma\gamma_\delta\}P_{1\alpha}P'_{1\beta}P''_{1\gamma}P'''_{1\delta}, \end{aligned} \tag{21}$$

with

$$P'_1 = P_1 - k', \quad P''_1 = P_1 - k' - q, \quad P'''_1 = P_1 - k. \tag{22}$$

The trace in (21) is a sum of 105 terms, each being a product of four Kronecker δ's containing pairs of all indices. The terms, where any pair of the letters μ,ν,λ,σ appears on the same Kronecker δ, do not contribute to the A's, and there remain 24 contributing terms. Collecting these terms we find the relevant contribution a_1^{ijlm} to A_1^{ijlm} from N_1^A, and after integration over d^4p,

$$\int \frac{d^4p}{(p^2 + D_1)^4} = \frac{i\pi^2}{6D_1{}^2},$$

the expression for A_1 becomes

$$A_1^{ijlm} = i\pi^2 \int d\tau\, a_1^{ijlm} D_1{}^{-2}, \tag{23}$$

where we have written

$$\int d\tau = \int_0^1 dx \int_0^x dy \int_0^y dz\,. \tag{24}$$

The a_1^{ijlm} are real polynomials in x, y, and z, and the relevant ones are given in Ref. 11 together with the corresponding coefficients a_3^{ijlm}; a_2^{ijlm} is not needed.

C. Integration over the momentum transfer $\vec{q}$

The Delbrück amplitude is now given as a sixfold integral by Eqs. (2), (3), (12), (16), and (23). We shall perform the integration over d^3q in (3).

Writing the amplitude a in the form

$$a = -ie_i e_j' P_{ij} = \sum_{n=1}^{3} P_n\,, \tag{25}$$

we find

$$P_n = \frac{im}{(2\pi)^3} \int \frac{d\tau}{\lambda_n^2} \int d^3q \frac{\vec{q}^2 A_n(\vec{q}) + B_n(\vec{q})}{\vec{q}^2 (\vec{q}-\vec{\Delta})^2 (\vec{q}^2 - 2\vec{q}\cdot\vec{Q}_n + \omega^2\lambda_n^2)^2}\,. \tag{26}$$

Here $A(\vec{q})$ and $B(\vec{q})$ are, when the index n is suppressed,

$$A(\vec{q}) = \alpha_1 \vec{e}\cdot\vec{q}\,\vec{e}'\cdot\vec{q} + \alpha_2 \vec{e}\cdot\vec{e}'\,\vec{k}\cdot\vec{q} + \alpha_3 \vec{e}\cdot\vec{k}'\,\vec{e}'\cdot\vec{q} - \alpha_2 \vec{e}'\cdot\vec{k}\,\vec{e}\cdot\vec{q} + \omega^2\alpha_4 \vec{e}\cdot\vec{e}' + \alpha_5 \vec{e}\cdot\vec{k}'\,\vec{e}'\cdot\vec{k}\,, \tag{27}$$

$$\begin{aligned} B(\vec{q}) = {}& \beta_1 \vec{e}\cdot\vec{e}'\,\vec{k}\cdot\vec{q}\,\vec{k}'\cdot\vec{q} + \omega^2\beta_2 \vec{e}\cdot\vec{q}\,\vec{e}'\cdot\vec{q} - \beta_1 \vec{e}'\cdot\vec{k}\,\vec{e}\cdot\vec{q}\,\vec{k}'\cdot\vec{q} - \beta_1 \vec{e}\cdot k'\,\vec{e}'\cdot\vec{q}\,\vec{k}\cdot\vec{q} + (\omega^2\beta_3 \vec{e}\cdot\vec{e}' + \beta_7 \vec{e}\cdot\vec{k}'\,\vec{e}'\cdot\vec{k})\vec{k}\cdot\vec{q} \\ & + (\omega^2\beta_4 \vec{e}\cdot\vec{e}' + \beta_8 \vec{e}\cdot\vec{k}'\,\vec{e}'\cdot\vec{k})\vec{k}'\cdot\vec{q} + \omega^2\beta_5 \vec{e}\cdot\vec{k}'\,\vec{e}'\cdot\vec{q} + \omega^2\beta_6 \vec{e}'\cdot\vec{k}\,\vec{e}\cdot\vec{q} + \omega^2\beta_9 \vec{e}\cdot\vec{k}'\,\vec{e}'\cdot\vec{k} + \omega^4\beta_{10} \vec{e}\cdot\vec{e}'\,. \end{aligned} \tag{28}$$

The coefficients α_i and β_i, which we really should have written α_i^n, β_i^n, follow from the a_n^{ijlm}. They are polynomials in x, y, and z, depend on the scattering angle θ, and are given in Appendix B for $n=1,3$.

We can now do the $\vec{q}$ integration in (26), where evidently the $B_n(\vec{q})$ terms are the most complicated ones. To simplify the denominator we introduce two Feynman parameters u and v, and we obtain integrals of the form

$$\int d^3q \{1; q_i; q_i q_j\} [(\vec{q}-\vec{q}_1)^2 + r_1^2]^{-4}\,,$$

which give

$$\pi^2 \{1; q_{1i}; q_{1i}q_{1j} + \delta_{ij} r_1^2/3\} (8 r_1^5)^{-1}\,.$$

Thus the final expression for P_n becomes

$$P_n = \frac{im}{16\pi\omega} \int \frac{d\tau}{\lambda_n^2} \{\vec{e}\circ\vec{e}'[\alpha_1 J_1^{(n)} + J_2^{(n)} + z_0 J_3^{(n)} + \tfrac{1}{2} J_4^{(n)}] + \vec{e}\cdot\vec{k}'\,\vec{e}'\cdot\vec{k}[J_5^{(n)} + z_1 J_3^{(n)} + \tfrac{1}{2} J_6^{(n)}]\}\,, \tag{29}$$

with the integrals (suppressing the superscript n)

$$\begin{aligned} J_1 &= \int_0^1 v\,dv\,M^{-1/2}\,, \\ J_2 &= \int_0^1 v\,dv\,(y_0 + y_1 v) M^{-3/2}\,, \\ J_3 &= \int_0^1 u^2 du \int_0^1 v\,dv\,L^{-3/2}\,, \\ J_4 &= \int_0^1 u^2 du \int_0^1 v\,dv [t_0 + t_1 u + t_2 u^2 \\ &\qquad + (t_3 + t_4 u)uv + t_5 u^2 v^2] L^{-5/2}\,, \\ J_5 &= \int_0^1 u^2 du \int_0^1 v\,dv\,(y_2 + y_3 v + y_4 v^2) M^{-3/2}\,, \\ J_6 &= \int_0^1 u^2 du \int_0^1 v\,dv [t_6 + t_7 u + t_8 u^2 \\ &\qquad + (t_9 + t_{10} u)uv + t_{11} u^2 v^2] L^{-5/2}\,, \end{aligned} \tag{30}$$

and the denominators

$$\begin{aligned} M &= v[h_1 + (1-v)h_2]\,, \\ L &= -h_2 u^2 v^2 + 2(h_4 u + h_3/2)uv + h_0 u(1-u)\,, \end{aligned} \tag{31}$$

where

$$\begin{aligned} & h_0 = 4\sin^2(\tfrac{1}{2}\theta)\,, \quad h_1 = \mu - \vec{Q}^2/\omega^2\,, \\ & h_2 = (\vec{Q} - \vec{\Delta})^2/\omega^2\,, \quad h_3 = \mu - \vec{\Delta}^2/\omega^2\,, \\ & h_4 = \vec{\Delta}\cdot(\vec{\Delta} - \vec{Q})/\omega^2\,. \end{aligned} \tag{32}$$

The remaining coefficients y_i, z_i, and t_i, which are functions of x, y, z, and θ, are given in Appendix B 4.

In the expression (29) for P_n we have so far only defined the relevant quantities for P_1 and P_3. Considering P_2, which originates from diagram b of Fig. 1, one might believe that P_2 equals P_1 since the complete integrated contributions from diagrams a and b evidently are equal. However, with our method P_2 is computed from the tensor

$\Pi_{\mu\nu\lambda\sigma}$ of Eq. (9) before it is allowed to set $\lambda=\sigma=4$, and consequently P_2 is different from P_1. As is shown in detail in Ref. 11 the difference is small, and P_2 is equal to P_1 given by (29), except that in the expression for J_2 in (30), $y_0^{(1)}$ and $y_1^{(1)}$ must be replaced by $y_0^{(2)}=\alpha_4^{(1)}+2\alpha_3^{(1)}S^2$, $y_1^{(2)}=\alpha_3^{(1)}Y'^{(1)}$ [cf. Eq. (B5)], respectively.

D. Real and imaginary parts, singularities

The formula (29) defines P_n as a three-dimensional integral over x, y, and z, and the integrand contains quantities J_i which themselves are one- or two-dimensional integrals over u, or u,v. The dependence of J_i on u and v is shown explicitly in (30) and (31), and it is seen that the integration over v is straightforward in all J_i's. It is possible also to perform the u integration analytically, but we did not find it convenient to do so since it would complicate considerably our numerical treatment of the remaining integrations. It is, however, convenient to separate the real and the imaginary parts of the scattering amplitude at this stage while we are still using analytical methods. It is seen from Eqs. (30) and (31) that the J_i's may have imaginary parts if the factors M and L which occur in the denominators are negative. More precisely, according to the usual prescription for defining imaginary parts by replacing the electron mass m by $m-i\epsilon$, where ϵ is small, the quantities M and L become complex, and the imaginary parts can be shown to be

$$\mathrm{Im}M=-2\epsilon m v(\lambda\omega^2)^{-1}, \quad \mathrm{Im}L=-2\epsilon m u v(\lambda\omega^2)^{-1}.$$

Non-negligible imaginary parts in the J's occur only where M and L have negative real parts. This condition is equivalent to $h_1\leq 0$ [cf. Eq. (32)], as may be seen after the v integration has been done in (30).

We now have to integrate the variables x, y, z, and u separately over the regions $h_1>0$ and $h_1<0$ [cf. Eq. (32)]. It is fairly easy to show that for photon energy $\omega<2m$ we always have $h_1>0$, that is, a real amplitude, but for $\omega>2m$ the relation $h_1=0$ defines quite complicated surfaces within the volume of integration. We shall not show these tedious calculations here. Details may be found in Ref. 11, where expressions for the real and the imaginary parts have been given explicitly.

We shall briefly discuss the singularities of the Delbrück amplitude since they are of interest for dispersion-relation calculations.[7] Singular points in the amplitude must originate in zeros in the factor $\vec{q}^2(\vec{q}-\vec{\Delta})^2(\vec{q}^2-2q\cdot\vec{Q}+\omega^2\mu)^2$ which appears in (26).

Since we have a three-dimensional integration over d^3q there is generally no singularity for $\vec{q}=0$ or $\vec{q}=\vec{\Delta}$. Singularities may occur, however, for $\vec{q}=0$ if $\vec{\Delta}=0$, or if $\omega^2\mu=0$, and for $\vec{q}=\vec{\Delta}$ if also $\Delta^2-2\vec{\Delta}\cdot\vec{Q}+\omega^2\mu=0$. Singularities will also occur for $\vec{q}=\vec{Q}$ if $\omega^2h_1=0$ since $\vec{q}^2-2\vec{q}\cdot\vec{Q}+\omega^2\mu=(\vec{q}-\vec{Q})^2+\omega^2h_1$.

We find that the case $\vec{\Delta}=0$ does not give any singularities since, if $\vec{\Delta}=0$, the numerator in (26) is proportional to $\vec{q}^2$ for small $\vec{q}$ [cf. Eq. (28)]. The cases $\omega^2\mu=0$ and $\vec{\Delta}^2-2\vec{\Delta}\cdot\vec{Q}+\omega^2\mu=0$ both lead to a singularity for

$$m^2+4\omega^2\sin^2(\theta/2)f(x,y,z)=m^2+\vec{\Delta}^2 f(x,y,z)=0, \tag{33}$$

where $f(x,y,z)$ is a function that varies between 0 and $\frac{1}{4}$. The case $\omega^2h_1=0$ leads to a branch point at $\omega=2m$. Thus the scattering amplitude as a function of complex ω^2 has a branch point at $\omega^2=4m^2$, and if the momentum transfer $\vec{\Delta}$ is a constant, this is the only singularity. However, if ω^2 varies for constant scattering angle θ, we find from (33) a branch point at $\omega^2=\omega_-^2=-2m^2(1-\cos\theta)^{-1}$. Using dispersion relations at constant θ we therefore have a right-hand cut beginning at $\omega^2=4m^2$, and at a left-hand cut beginning at $\omega^2=\omega_-^2$. The latter has not been taken into account in the calculations of Ehlotzky and Sheppey.[7]

E. The numerical calculation

It follows from (29) and (30) that after the v integration in (30) has been performed analytically, and the real and the imaginary parts of the amplitude have been separated, we are left with four-dimensional integrals. These are integrated numerically by the method of Gaussian quadrature. The integrand in (29) is not suited for immediate numerical treatment since cancellations between individually divergent terms occur, and inconvenient square-root factors, such as $\sqrt{u}$, also appear in the denominators. These factors may be eliminated by a change of variables, and the cancellations can be taken care of analytically. After these modifications the numerical integration works well, especially near the forward direction where it is sufficient to compute the integrand for only about $N=300$ different combinations of values of the four variables to obtain an accuracy better than 5%. The accuracy is estimated by observing the convergence of the results as the number N increases.

As the scattering angle is increased, particularly at high energies, complications increase because there are large cancellations between terms originating from diagrams (a), (b), and (c) of Fig. 1, respectively. We were, however, able to calculate the amplitude for all values of energy and angle that were of interest to us, but since a typical time for one calculation of the integrand was

0.03 sec on the UNIVAC 1108 computer, we evidently could not aim for a systematic tabulation of the cross section. Selected values of the Delbrück amplitude are given in Sec. III.

III. RESULTS

We shall express our results in terms of the amplitudes for linear polarization, and we therefore discuss the polarization formalism first.

A. The description of polarization

The Delbrück amplitude a is, according to (25) and (29), of the form

$$a = f\vec{e}\cdot\vec{e}\,' + g\vec{e}\cdot\vec{k}\,'\vec{e}\,'\cdot\vec{k}\,, \tag{34}$$

where $\vec{e}$ and $\vec{e}\,'$ are polarization vectors for linear polarization, and f and g are functions of ω and θ. This form is obvious since a is linear in $\vec{e}$ and $\vec{e}\,'$, and the only other vectors in the problem are $\vec{k}$ and $\vec{k}\,'$. It is convenient[5] to choose the polarization vectors either in or orthogonal to the scattering plane. We then have only two nonzero amplitudes,

$$\begin{aligned} a_\perp &= f\,, \\ a_\parallel &= f\cos\theta - g\sin^2\theta\,, \end{aligned} \tag{35}$$

where $a_\perp$ is the amplitude for the case where $\vec{e}=\vec{e}\,'$ and both are orthogonal to the scattering plane, and $a_\parallel$ is the amplitude when both $\vec{e}$ and $\vec{e}\,'$ are in this plane. The unpolarized cross section is from (1),

$$\frac{d\sigma}{d\Omega} = \tfrac{1}{2}(\alpha Z)^4 r_0^2(|a_\perp|^2 + |a_\parallel|^2)\,. \tag{36}$$

To describe circular polarization we use the complex vectors

$$\vec{e}_\pm = (\vec{e}_1 \pm i\vec{e}_2)/\sqrt{2}\,, \tag{37}$$

where $\vec{e}_1$ and $\vec{e}_2$ are the linear polarization vectors in or orthogonal to the scattering plane, respectively. There are four helicity amplitudes, a_{++}, a_{+-}, a_{-+}, and a_{--}, where a_{++} is obtained from (34) with $\vec{e}=\vec{e}_+$ and $\vec{e}\,'=\vec{e}_+'^{\,*}$, and the other amplitudes are defined similarly. It is easily shown that the spin-nonflip amplitudes are

$$a_{++} = a_{--} = \tfrac{1}{2}(a_\parallel + a_\perp)\,, \tag{38}$$

while the spin-flip amplitudes are

$$a_{+-} = a_{-+} = \tfrac{1}{2}(a_\parallel - a_\perp)\,. \tag{39}$$

B. The very low and the very high energy regions

In order to check our calculations with known results we performed analytically the integrations of the amplitude for the low-energy case, $\omega \ll m$, and for the case of high energies in the forward direction, $\omega \gg m$, $\theta=0$.

The nonrelativistic amplitude is real, and by straightforward expansion in powers of ω/m we find that the coefficients of the terms of the two lowest orders vanish, so the amplitude is of order ω^2. Elementary integrations[11] give for the quantities f and g in (34)

$$\begin{aligned} f &= \omega^2(59 + 14\cos\theta)(32\times 72m^2)^{-1}\,, \\ g &= -14\omega^2(32\times 72m^2)^{-1}\,, \end{aligned} \tag{40}$$

which confirms the results of Costantini *et al.*[8]

For the forward direction the cross section is given by $a_\perp = f$ alone, and for $\omega \gg m$ we have $\mathrm{Im}f \gg \mathrm{Re}f$, so we only have to calculate $\mathrm{Im}f$. The calculation is not very difficult, and we recover the known expression, first obtained by Rohrlich and Glückstern,[4]

$$a = \mathrm{Im}f = \frac{7\omega}{9\pi m}\left(\ln\frac{2\omega}{m} - \frac{109}{42}\right), \tag{41}$$

which is proportional to the pair-production total cross section, as is well known.

C. Numerical results, low energy

Since the low-energy cross section is well established, calculations in this energy region furnished a convenient test for the numerical program. We computed the linear polarization amplitudes $a_\perp$ and $a_\parallel$ defined by Eqs. (34) and (35), and in Table I we show a comparison of our values for $\mathrm{Re}a$ with the values obtained from the low-energy formula (40) for the forward direction. Note that $a=a_\perp=a_\parallel$ for $\theta=0$, and that a is real for $\omega<2m$. It is seen that the low-energy formula gives surprisingly good results also for $\omega=2m$.

In Figs. 2 and 3 we show the angular distribution of $a_\perp$ and $a_\parallel$, respectively, for some energies $\omega<m$. For large-angle scattering we have a considerable departure from the low-energy approximation (40) already for $\omega \gtrsim 0.1m$. Note that $a_\perp > a_\parallel$ for $\omega<m$, while this inequality is reversed for $\omega>m$ for almost all scattering angles.

D. Numerical results, intermediate energy

In the following we show some results for the Delbrück amplitude for photon energies $\omega = 1.33$,

TABLE I. The forward Delbrück amplitude a_{num} which is calculated numerically, and the low-energy approximation $a_{\mathrm{le}} = 73\omega^2(72\times 32m^2)^{-1}$. The photon energy is ω.

ω/m	$\mathrm{Re}a_{\mathrm{num}}$	a_{le}
0.2	1.27×10^{-2}	1.27×10^{-2}
1.0	3.16×10^{-2}	3.17×10^{-2}
2.0	0.13	0.127
2.6	0.241	0.214

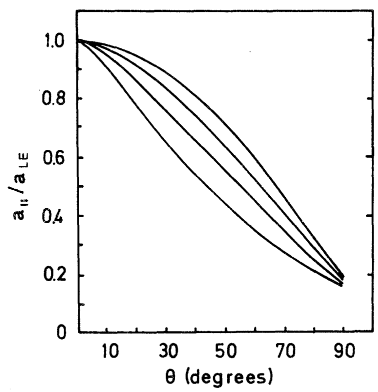

FIG. 2. The angular dependence of the Delbrück amplitude $a_{\parallel}$. The forward low-energy approximation a_{le} is given in Table I. From the upper to the lower curve $\omega/m=0$, 0.2, 0.5, and 1.0, respectively.

TABLE II. Real parts of $a_{\perp}$ and $a_{\parallel}$ for $\omega=1.33$ MeV as a function of the scattering angle θ.

θ (deg)	Re$a_{\perp}$	Re$a_{\parallel}$	θ (deg)	Re$a_{\perp}$	Re$a_{\parallel}$
10	0.170	0.179	90	0.000	0.026
20	0.119	0.134	100	−0.004	0.023
30	0.080	0.098	110	−0.007	0.020
40	0.053	0.074	120	−0.010	0.018
50	0.035	0.057	125	−0.010	0.017
60	0.024	0.045	130	−0.010	0.015
70	0.011	0.036	140	−0.011	0.014
80	0.005	0.030			

7.9, 9.0, 10.83, 15.1, and 87 MeV. These values have been chosen since they are relevant for actual experiments. Comparisons with the experiments are shown in the next section.

In Table II the real parts of $a_{\parallel}$ and $a_{\perp}$ are given for $\omega=1.33$ MeV. Imaginary parts are negligible for this energy. In Table III $a_{\parallel}$ and $a_{\perp}$ are given for $\omega=7.9$ MeV, and in Tables IV–VII these quantities are given for $\omega=9.0$, 10.83, 15.1, and 87 MeV, respectively.

The numbers in Table II have an accuracy of about 5–10%. This also applies to the imaginary parts given in Table V, while the real parts are accurate within 10% for scattering angles below 10°, but the error might be of order 20% for larger angles. The accuracy in Tables III, IV, VI, and VII is about 10% for all numbers, where errors are not explicitly given.

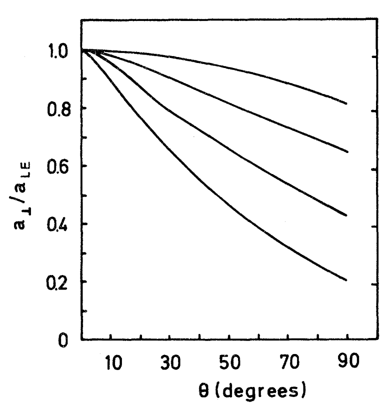

FIG. 3. The angular dependence of $a_{\perp}$ (cf. Fig. 2). From the upper to the lower curve $\omega/m=0$, 0.2, 0.5, and 1.0, respectively.

The results for ω smaller than 20 MeV can be compared with the numbers obtained by Ehlotzky and Sheppey.[7] The imaginary parts are in good agreement with our results, but the real parts disagree. This was to be expected since Ehlotzky and Sheppey, in their dispersion relation, neglected the contribution from the left-hand cut, which was discussed in Sec. II D above.

E. Numerical results, high energy

For high energies the forward asymptotes were first calculated by Rohrlich and Glückstern.[4] The imaginary part of the amplitude is given by (41), while the real part is smaller by a factor of $\ln\omega$. Later Cheng and Wu[9] obtained the approximations

$$\mathrm{Im}a_{\perp}=Z\omega[\ln(m/\Delta)+\tfrac{19}{21}](9\pi m)^{-1}, \tag{42}$$

$$\mathrm{Im}a_{\parallel}=\mathrm{Im}a_{\perp}+\omega(9\pi m)^{-1}, \tag{43}$$

valid for momentum transfer Δ in the region

$$(m^2/\omega)\ll\Delta\ll m, \tag{44}$$

while

$$\mathrm{Im}a_{\perp}=1.18(\omega/m)(\Delta/m)^{-2}, \tag{45}$$

$$\mathrm{Im}a_{\parallel}=2.46(\omega/m)(\Delta/m)^{-2}, \tag{46}$$

for

$$m\ll\Delta\ll\omega. \tag{47}$$

We tried to check these formulas. In Table VIII we show values of the forward amplitude a compared with the approximate a_{he} of Eq. (41). It is seen that they approach each other rapidly, and within our accuracy they are equal for $\omega\gtrsim 40$ MeV.

In order to check (42) we chose the momentum transfer to be

$$\Delta=m(m/\omega)^{1/2}, \tag{48}$$

and the corresponding values for Im$a_{\perp}$ found by numerical integration and from (42) are shown

TABLE III. The quantities $a_\perp$ and $a_\parallel$ for photon energy $\omega = 7.9$ MeV.

θ (deg)	Re$a_\parallel$	Im$a_\parallel$	Re$a_\perp$	Im$a_\perp$
25	0.154	0.221	0.068	0.063
35	0.094	0.124	0.035	$(2.4 \pm 0.3) \times 10^{-2}$
45	0.064	0.077	0.0189×10^{-2}	$(9 \pm 2) \times 10^{-3}$
60	0.040	0.044	$(8 \pm 1) \times 10^{-3}$	$(5 \pm 10) \times 10^{-4}$
75	0.026	0.027	$(1.8 \pm 0.7) \times 10^{-3}$	-4.5×10^{-3}
90	0.0183	0.0184	$-(1.7 \pm 0.5) \times 10^{-3}$	-6.2×10^{-3}
120	1.07×10^{-2}	1.10×10^{-2}	-5.2×10^{-3}	-7.4×10^{-3}
140	8.32×10^{-3}	8.9×10^{-3}	-6.2×10^{-3}	-7.6×10^{-3}

in Table IX. Apparently the convergence to the asymptotic limit is very slow, but this conclusion is not definite since it is difficult to give a precise estimate of the accuracy; it is certainly better than 10%.

We also computed the difference $\mathrm{Im}(a_\parallel - a_\perp)$. For Δ given by (48), Eq. (44) gives $\mathrm{Im}(a_\parallel - a_\perp) = \omega(9\pi m)^{-1}$, and since now $\theta \approx (m/\omega)^{3/2}$, Eq. (35) yields $a_\parallel - a_\perp \approx -g \sin^2\theta$. The results are shown in Table X, and it is again seen that the convergence to the asymptotic limit is slow. It should be noted that polarization effects are very small at these angles and little dependent on energy since $\mathrm{Im}(a_\parallel - a_\perp)(\mathrm{Im}a_\perp)^{-1}$ is small (approximately $\frac{1}{30}$), and almost energy independent.

The high-energy intermediate momentum transfer region defined by (47) could not easily be reached with our method. With

$$\Delta = m(\omega/m)^{1/2} \tag{49}$$

and $\omega = 1920$ MeV formula (45) gives $\mathrm{Im}a_\perp = 1.18$ while we find $\mathrm{Im}a_\perp = 1.33$. The difference is not significant since it is smaller than our estimated error. Since more than four minutes was spent on the computer for just this calculation we did not pursue the computation in this region.

III. COMPARISON WITH EXPERIMENTS

In actual experiments Delbrück scattering is produced in the Coulomb field of atomic nuclei. Since these have finite mass M, nuclear Compton scattering is possible, and we may also have Rayleigh and nuclear resonance scattering. All these effects are coherent and cannot be separated experimentally, except for high energies where Delbrück scattering dominates. We shall not go into details here. Except for nuclear Compton scattering which reduces to the very simple Thomson amplitude [cf. Eq. (1)],

$$A_{\mathrm{Th}} = -r_0 \frac{Z^2 m}{M} \vec{e} \cdot \vec{e}\,' , \tag{50}$$

the theory for the other processes is quite complicated and far from complete. We only refer to the discussion in Ref. 11 and in the experimental articles of Basavaraju and Kane,[14] Schumacher *et al.*,[15] Hardie *et al.*,[16] Kahane and Moreh,[17] and Jackson *et al.*[18] In the experiments of Moffat and Stringfellow[19] and Jarlskog *et al.*[20] the photon energy is high, and Delbrück scattering therefore dominates. The experiments mentioned here are selected because they are the most accurate tests of the Delbrück process.

Basavaraju and Kane,[14] and later Schumacher *et al.*[15] measured the Delbrück cross section at

TABLE IV. Real parts of $a_\perp$ and $a_\parallel$ for $\omega = 9$ MeV.

θ (deg)	Re$a_\perp$	Re$a_\parallel$
25	0.065	0.145
35	0.033	0.088
45	0.018	0.059
60	$(6.8 \pm 2.0) \times 10^{-3}$	0.036
75	$(1.3 \pm 1.0) \times 10^{-3}$	0.023
90	$(-1.75 \pm 0.50) \times 10^{-3}$	0.017
120	-0.0046	0.0096
140	-0.0055	0.0074

TABLE V. The quantities $a_\perp$ and $a_\parallel$ for $\omega = 10.83$ MeV.

θ (deg)	Re$a_\perp$	Im$a_\perp$	Re$a_\parallel$	Im$a_\parallel$
0.01	6.54	6.52	6.54	6.52
0.5	4.73	6.03	4.99	6.17
1.0	3.55	5.15	3.88	5.48
1.5	2.71	4.33	3.04	4.78
2.0	2.15	3.64	2.46	4.17
3.0	1.51	2.59	1.79	3.20
5.0	0.80	1.39	1.02	2.00
10	0.26	0.41	0.41	0.85
15	0.13	0.17	0.23	0.46
20	0.097	0.090	0.17	0.29
25	···	0.05	···	0.20
30	0.036	0.036	0.086	0.15
40	0.026	0.014	0.064	0.08
50	0.012	0.005	0.039	0.053
70	0.0034	-0.002	0.023	0.03
90	-6×10^{-4}	-0.005	0.014	0.015
120	-0.0047	-0.007	0.0086	0.0093
150	-5.3×10^{-3}	-7×10^{-3}	6.2×10^{-3}	7.4×10^{-3}

TABLE VI. The quantities $a_\perp$ and $a_\parallel$ for $\omega = 15.1$ MeV.

θ (deg)	Re$a_\perp$	Im$a_\perp$	Re$a_\parallel$	Im$a_\parallel$
10	0.21	0.32	0.29	0.80
20	0.061	0.075	0.125	0.26
40	0.011	0.013	0.041	0.073
60	1.5×10^{-3}	8×10^{-4}	0.021	0.030
75	-8×10^{-4}	-2.6×10^{-3}	0.014	0.018
90	-2.1×10^{-3}	-4.1×10^{-3}	0.010	0.012
120	-3.7×10^{-3}	-4.6×10^{-3}	6.4×10^{-3}	6.9×10^{-3}
150	-4.5×10^{-3}	-4.2×10^{-3}	5.0×10^{-3}	4.7×10^{-3}

$\omega = 1.33$ MeV. At this energy the amplitude has only a small imaginary part, and for scattering angles larger than 90° the spin-flip amplitudes A_{+-} of Rayleigh and Delbrück scattering should interfere destructively. For the latter process Basavaraju and Kane give Re$A_{+-} = -0.0060 r_0$ for $Z = 82$, $\theta = 120°$, while Schumacher *et al.* find Re$A_{+-} = -(0.0090 \pm 0.0020) r_0$ for $Z = 82$, $\theta = 150°$. From Table II we find that $A_{+-} = (\alpha Z)^2 r_0 a_\parallel$ is Re$A_{+-}/r_0 = 0.0048$, 0.0050, 0.0045, and 0.0045 for $Z = 82$, and for $\theta = 110°$, 120°, 130°, and 140°, respectively. The disagreement with the experiments is evident.

Also Hardie *et al.*[16] made their experiment at $\omega = 1.33$ MeV. We are grateful to Professor Hardie who provided us with the Rayleigh amplitudes calculated by his group. Using these values, the Thomson amplitude (50), and our Table II we find the scattering cross section shown in Fig. 4. For comparison we also show the theoretical cross section if the Delbrück process is neglected and the experimental values. It is seen that while the inclusion of Delbrück scattering definitely improves the agreement between theory and experiment for θ smaller than 60°, we have considerable discrepancies at larger angles. Note that for $\theta = 120°$ the spin-flip Rayleigh amplitude dominates. The Thomson amplitude is about half of it while the Delbrück amplitude contributes only about 10%. At the present stage of the theory for Rayleigh scattering it is therefore likely that the discrepancies between theory and experiment for large angles at $\omega = 1.33$ MeV are due to errors in the Rayleigh amplitude.

We next consider the experiment at $\omega = 7.9$ MeV of Kahane and Moreh.[17] At this energy and higher

TABLE VII. The quantities $a_\perp$ and $a_\parallel$ for $\omega = 87$ MeV.

θ ($m_{\rm rad}$)	Re$a_\perp$	Im$a_\perp$	Re$a_\parallel$	Im$a_\parallel$
1	⋯	96	⋯	101
1.89	13.9	75	14.9	81
3	⋯	59	⋯	65
4.24	7.7	47	8.1	53

TABLE VIII. The forward Delbrück amplitude a and the high-energy approximation $a_{\rm he}$ given by (41) for photon energy $\omega = 21.2m$ and $34.5m$.

ω/m	Rea	Re$a_{\rm he}$	Ima	Im$a_{\rm he}$
21.2	6.55	5.99	6.53	5.98
34.5	11.87	11.17	14.5	13.93

energies Rayleigh scattering is negligible, and for angles below about 80° Delbrück scattering gives the dominant contribution to the cross section. Now Kahane and Moreh find that the best fit to their experiment is obtained if the real part of the Delbrück amplitude is zero. Comparing with the real parts given in Ref. 7 they find a considerable disagreement. As is seen from Table III the real parts obtained by us are not negligible. In Fig. 5 we show a comparison between the experiment and our theory. We see that while for the element Ta the agreement is quite good for all angles, the experimental values are consistently (but not much) below the theoretical ones for Th and U for θ smaller than 90°.

In an experiment at $\omega = 10.83$ MeV Jackson *et al.*[18] have obtained good agreement with the theory. At the time this experiment was published our Delbrück results were available only for $\theta \leq 90°$, as may be seen from Figs. 5 and 6 in Ref. 18. Using Table V we now find theoretical values also for $\theta = 120°$ and 150°, and in Fig. 6 we show extended versions of the figures just mentioned. For lead the agreement between theory and experiment is very good except for $\theta = 50°$ and 60°, where there is an unexplained bump in the experimental cross section. The agreement is good also for uranium except that the theory seems to give too low values for large angles. In particular, we note that the real part of the Delbrück

TABLE IX. The small-angle Delbrück amplitude $a_\perp$ calculated numerically and $a_\perp^{\rm CW}$ calculated by Cheng and Wu [cf. Eq. (42)]. The momentum transfer is $\Delta = m(m/\omega)^{1/2}$.

ω/m	Im$a_\perp$	Im$a_\perp^{\rm CW}$
275	212	252
4[illegible]	334	386
1000	990	1080
2000	2200	2340
3000	3480	3650
4000	4800	5010
7000	8930	9250
10 000	13 200	13 700
20 000	28 100	29 000
30 000	43 600	45 000

TABLE X. The difference $a_{\parallel} - a_{\perp}$ calculated for small momentum transfers $\Delta = m(m/\omega)^{1/2}$ as a function of photon energy ω. The Cheng and Wu results $(a_{\parallel} - a_{\perp})^{CW}$ are obtained from (43).

ω/m	$\mathrm{Im}(a_{\parallel} - a_{\perp})$	$\mathrm{Im}(a_{\parallel} - a_{\perp})^{CW}$
275	6.8	9.7
400	10.7	14.1
800	23.7	28.3
1000	30.5	35.3
1500	47.4	53
2000	64.4	70.5
3000	99	105
4000	134	141

amplitude is essential in order to obtain agreement at the smaller angles.

The results of Kahane and Moreh[17] and Jackson *et al.*[18] do not give a definite answer with respect to the real part of the Delbrück amplitude. In a private communication Moreh has very recently informed us that his group is obtaining new results at $\omega = 9$ MeV. We have calculated the real part of the Delbrück amplitude for this energy (Table IV), and we hope that this experiment will help to solve the problem of the real part.

Moffat and Stringfellow[19] performed a Delbrück experiment on uranium for $\omega = 87$ MeV and scattering angles $\theta = 1.89$ mrad and 4.24 mrad. They derived the cross section in two ways (in order to subtract the background), first by assuming Z^4 dependence of the cross section and then, in a less reliable way, by assuming an angular distribution suggested by Bethe and Rohrlich.[21] The results are shown in Table XI together with our theoretical numbers. The agreement is not very good, but the accuracy is not sufficient for any definite conclusion.

We finally mention the experiment of Jarlskog *et al.*[20] at photon energies from about 1 to 7 GeV. As has been shown by Cheng and Wu[9] Coulomb corrections are very important for this case, and our calculations are only useful as a check of the high-energy approximation of the lowest-order (in Z) cross section (cf. Sec. IIID).

The fact that Coulomb corrections are large at high energies and momentum transfers $\Delta \gg m$ casts some doubts on the usefulness of the lowest-order Delbrück cross section also at lower energies. Generally one should expect Coulomb corrections to increase with the momentum transfer since small impact parameters imply strong fields. It is therefore natural that the correction to the high-energy forward amplitude is small, as was first noticed by Rohrlich.[22] This amplitude is proportional to the pair-production total cross section, which gets its main contributions at high

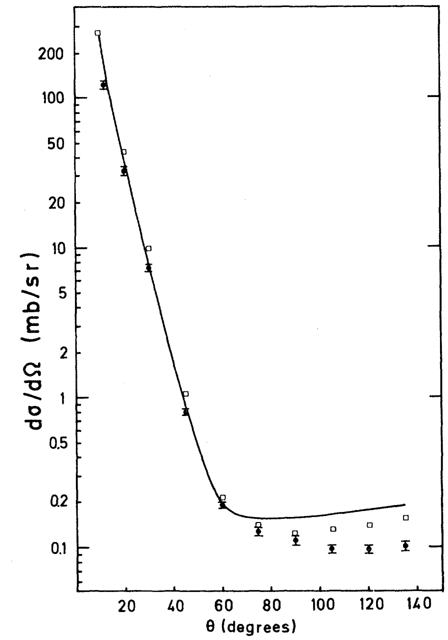

FIG. 4. Elastic scattering of 1.33-MeV photons by a lead target. The solid line is the calculated cross section with the values of Table II for the Delbrück amplitude, while the open squares give the calculated cross section if this amplitude is suppressed. The full circles with error bars give the experimental cross section of Hardie *et al.* (see Ref. 16).

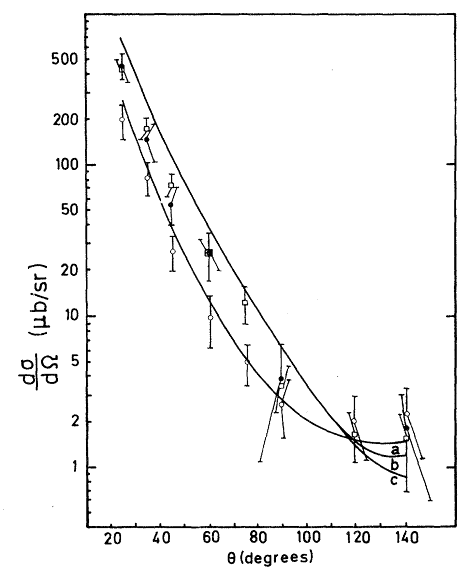

FIG. 5. Elastic scattering of 7.9-MeV photons. The theoretical cross section (solid lines) is compared with the measurements of Kahane and Moreh (see Ref. 17). In the figure the curves a, b, and c refer to targets of tantalum $Z = 73$, thorium $Z = 90$, and uranium $Z = 92$, and the corresponding experimental values are shown by open circles, solid circles, and open squares, respectively.

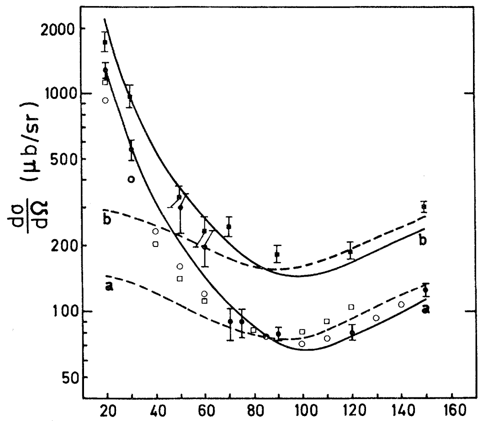

FIG. 6. Elastic scattering of 10.83-MeV photons. The solid circles and squares with error bars give the experimental cross section of Jackson *et al.* (see Ref. 18) for targets of lead and uranium, respectively. The solid lines a and b show the theoretical cross sections, respectively, for these materials. The dashed lines a and b are the calculated cross sections with the Delbrück amplitudes suppressed. The cross section for lead is also shown, by open circles when only the real parts of these amplitudes are suppressed, and by open squares when the amplitudes of Ehlotzky and Sheppey (see Ref. 7) are used.

energies from low momentum transfers. In this connection it should be noted that because of the intimate relation between the pair-production cross section and the Delbrück amplitude,[5] one should expect large Coulomb corrections in high-energy

TABLE XI. Delbrück experimental and theoretical values for the quantity $a^2 = (d\sigma/d\Omega)(\alpha Z)^{-4} r_0^{-2}$ at $\omega = 87$ MeV. Our calculations give $a_{\rm th}^2$; a_{E1}^2 and a_{E2}^2 are derived experimentally by Moffat and Stringfellow (see Ref. 19) by assuming a Z^4 dependence or a Bethe-Rohrlich-type (see Ref. 21) angular dependence of the cross section, respectively.

θ ($m_{\rm rad}$)	$a_{\rm th}^2$	a_{E1}^2	a_{E2}^2
1.89	6300 ± 630	5175 ± 497	6827 ± 616
4.24	2580 ± 260	1112 ± 200	2167 ± 196

wide-angle pair production (and bremsstrahlung) experiments on high-Z nuclei.

If we use the Coulomb corrections to the pair-production cross section as an indicator of the corrections to the imaginary part of the Delbrück amplitude, then the exact pair-production calculations of Øverbø, Mork, and Olsen[23] imply that considerable positive corrections may occur for low energies, ω about 1–2 MeV. The corrections should decrease with increasing energy, having a minimum in absolute value at about 5–6 MeV. However, it seems to be very difficult to give even a rough estimate of the corrections for the general case.

ACKNOWLEDGMENT

We wish to thank Professor Haakon Olsen, who introduced us to the problem, for his support. We also thank Dr. Jørgen Løvseth, who provided a tested procedure for Gaussian quadrature.

APPENDIX A: ELIMINATION OF THE COEFFICIENTS B AND C

Gauge invariance implies that

$$k_\mu^{(1)} \Pi_{\mu\nu\lambda\sigma} = 0 \,, \tag{A1}$$

where $\Pi_{\mu\nu\lambda\sigma}$ is the vacuum-polarization tensor. Inserting the expression (9) we find

$$\sum_{i=1,2;\, j,l,m=1,2,3} A^{ijlm} (k^{(1)} k^{(i)}) k_\nu^{(j)} k_\lambda^{(l)} k_\sigma^{(m)} + \sum_{l,m=1}^{3} (B_1^{lm} k_\nu^{(1)} k_\lambda^{(l)} k_\sigma^{(m)} + B_2^{lm} k_\nu^{(l)} k_\lambda^{(1)} k_\sigma^{(m)} + B_3^{lm} k_\nu^{(l)} k_\lambda^{(m)} k_\sigma^{(1)})$$
$$+ \sum_{i=2,3;\, l=1,2,3} (k^{(1)} k^{(i)}) (B_4^{il} \delta_{\nu\lambda} k_\sigma^{(l)} + B_5^{il} \delta_{\nu\sigma} k_\lambda^{(l)} + B_6^{il} \delta_{\lambda\sigma} k_\nu^{(l)}) + C_1 k_\nu^{(1)} \delta_{\lambda\sigma} + C_2 k_\lambda^{(1)} \delta_{\nu\sigma} + C_3 k_\sigma^{(1)} \delta_{\nu\lambda} = 0 \,. \tag{A2}$$

This equation leads to 36 relations between the A's, the B's, and the C's, since the 27 coefficients of the $k_\mu^{(i)} k_\lambda^{(j)} k_\sigma^{(k)}$ must vanish separately for all different values of i, j, and k, and also the nine coefficients of $k_\nu^{(i)} \delta_{\lambda\sigma}$ must vanish for all values of i and all three different permutations of ν, μ, and σ.

In the same way we can derive 72 additional relations from the identities

$$k_\nu^{(2)} \Pi_{\mu\nu\lambda\sigma} = k_\lambda^{(3)} \Pi_{\mu\nu\lambda\sigma} = 0 \,. \tag{A3}$$

Fortunately, we only need a small number of these relations to eliminate the nine B and C coefficients appearing in (11). In picking relations for these eliminations we shall take care to avoid relations which will introduce additional factors of $q = k^{(3)}$ in the denominators in the terms of the integrand in Eq. (3), and possible convergence difficulties.

The relations following from (A2) are of the type

$$(k^{(1)}k^{(2)})A^{2112}+(k^{(1)}k^{(2)})A^{3112}+B_1^{12}+B_2^{12}=0\ ,$$

and from a total of 17 such identities (see Ref. 11 for further details) we obtain

$$\begin{aligned}
&B_1^{11}=-p^{12}A^{2111}-p^{23}A^{2311}, \quad B_1^{12}=-p^{12}A^{2112}+p^{23}A^{3122}+p^{33}A^{3132},\\
&B_1^{21}=-p^{12}A^{2121}+p^{13}A^{2311}+p^{33}A^{2331}, \quad B_1^{22}=-p^{12}A^{2122}-p^{13}A^{3122},\\
&B_6^{21}=-p^{13}A^{2113}-p^{23}A^{2123}-p^{33}A^{2133}, \quad B_6^{23}=-p^{13}(A^{2313}+A^{3123})-p^{33}A^{2333},\\
&B_6^{31}=-p^{23}(A^{2313}+A^{3123})-p^{33}A^{3133}, \quad B_6^{33}=p^{12}(A^{2313}+A^{3123})-p^{33}A^{3333},\\
&C_1=p^{12}p^{13}A^{2113}+p^{12}p^{23}A^{2123}+p^{12}p^{33}A^{2133}+p^{13}p^{23}(A^{2313}+A^{3123})+p^{13}p^{23}A^{3133},
\end{aligned} \tag{A4}$$

with $p^{ij}=k^{(i)}k^{(j)}$. Inserting (A4) into (11) we get (12).

APPENDIX B

1. The functions $l_i^{(i)}, \lambda_i, \mu_i, \kappa_i, \kappa_i'$

The denominator in Eq. (7) is a product of the factors

$$a_1=p^2+m^2, \quad a_2=(p-k')^2+m^2, \quad a_3=(p-k'-q)^2+m^2, \text{ and } a_4=(p-k)^2+m^2,$$

and when Feynman parameters x, y, and z are introduced a new denominator

$$[a_1z+a_2(y-z)+a_3(x-y)+a_4(1-x)]^4$$

appears. In (17) this is written as $[(p-P_1)^2+D_1]^4$. Straightforward calculations give

$$\begin{aligned}
&l_1^{(1)}=1-x, \quad l_2^{(1)}=x-z, \quad l_3^{(1)}=x-y, \quad \lambda_1=(x-y)(1-x+y), \quad \kappa_1=(1-x)(1-x+y)^{-1}\ ,\\
&\kappa_1'=(1-x+z)(1-x+y)^{-1}, \quad \mu_1=[m^2+4\omega^2\sin^2(\theta/2)(1-x)(x-z)](\lambda_1\omega^2)^{-1}\ .
\end{aligned} \tag{B1}$$

Using (7) and (15) we find in the same way for $T^{(3)}_{\mu\nu\lambda\sigma}$

$$\begin{aligned}
&l_1^{(3)}=(1-x), \quad l_2^{(3)}=z, \quad l_3^{(3)}=y, \quad \lambda_3=y(1-y),\\
&\kappa_3=(1-x)(1-y)^{-1}, \quad \kappa_3'=z/y, \quad \mu_3=[m^2+4\omega^2\sin^2(\theta/2)z(1-x)](\lambda_3\omega^2)^{-1}\ .
\end{aligned} \tag{B2}$$

2. The α_i^1 and β_i^1 (the superscript is omitted below)

We use the notation $x'=(1-x)$, $y'=(1-y)$, $z'=(1-z)$, $t=x-y$, $t'=1-t$, $s=x-z$, $s'=1-s$, $S=\sin(\theta/2)$. Then the coefficients α_i^1 and β_i^1 are

$$\begin{aligned}
&\alpha_1=32t't^3\ , \quad \alpha_2=-32x't^2t'\ , \quad \alpha_3=32st^2t'\ , \quad \alpha_4=8t(1-2t)(xs'+3x's)+2\alpha_5S^2\ , \quad \alpha_5=-8tt'(1-4x's)\ ,\\
&\beta_1=-32x'ts(1-2t)+8x't(1-4t)-8ts'\ , \quad \beta_2=-16x't^2(x'-z)+16t^2(x'-2z)s'-2\beta_1S^2\ ,\\
&\beta_3=-8x't(1-2s+4x's)-8ts'(1-2x'+4x's)+16S^2x'[x's(1-3t)-xst'+ts']\ ,\\
&\beta_4=8x't(1-2s+4x's)-8ts'(1-2x'+4x's)-16S^2[xtss'+x'(1-3t)ss'+ts'^2-x's^2]\ ,\\
&\beta_5=-16x'ts^2+40x'tss'+8ts'^2-8x't(1-2s+4x's)-8tss'(2-3x+4z)\ ,\\
&\beta_6=8zt[(x'-z)(1-2x)+s(3-2x)]\ , \quad \beta_7=8x'^2s(1-3t)+8x'(ts'-xt's)\ ,\\
&\beta_8=-8xtss'-8x'(1-3t)ss'-8ts'^2+8x's^2\ , \quad \beta_9=-32z^2x's\ , \quad \beta_{10}=2\beta_9S^2\ .
\end{aligned} \tag{B3}$$

3. The α_i^3 and β_i^3 (the superscript is omitted below)

The notation is as in Appendix B 2:

$$\begin{aligned}
&\alpha_1=-32y^2y'^2\ , \quad \alpha_2=-32y^2y'x'\ , \quad \alpha_3=-32yy'^2z\ , \quad \alpha_4=64yy'x'z-16y^2s+8y(2-3z)-8[yx'+z(1-2x)]+2S^2\alpha_5\\
&\alpha_5=-8yy'(1-4zx')\ , \quad \beta_1=-64yy'zx'-8x'(y-2z)-8zy'\ , \quad \beta_2=-32yy'ss'-2S^2\beta_1\ ,\\
&\beta_3=-32yzx'(x'-z)+16zx'(1-2x)-8zy'-8yx'+16S^2x'[zx'(1-2y)+yx'(1-2z)-xzy'+xyz']\ ,\\
&\beta_4=32yzx'(x'-z)-16zx'(1-2x)+8yx'+8zy'+16S^2z[yx'(1-2z)+zy'(2-3x)-xy'z']\ ,\\
&\beta_5=-8yx'(1+z)-8z^2x'(4y-5)+8zy'(1-2z)(x-2z)-8zx'[z'(1-2y)-2y'(1-2x)]\ ,\\
&\beta_6=-8yzx'(3-6x+4z)-8yx'(1-2x)(1-2x+z)+8zy'\ , \quad \beta_7=8zx'^2(1-2y)+8yx'^2(1-2z)-8xx'y'z+8xx'yz'\ ,
\end{aligned} \tag{B4}$$

$$\beta_8 = 8yx'z(1-2z) + 8z^2y'(2-3x) - 8xy'zz' , \quad \beta_9 = 32zx'ss' , \quad \beta_{10} = 2S^2\beta_9 .$$

4. The coefficients y_i, z_i, and t_i

With α, β, S, κ, and κ' given above, and $Y = \kappa - 1 - (\kappa' - 1)\cos\theta$, $Y' = \kappa' - 1 - (\kappa - 1)\cos\theta$ we have

$$\begin{aligned}
&z_0 = (\beta_2 + \beta_1 \cos\theta)/2 , \quad z_1 = -\beta_1 , \quad y_0 = \alpha_4 + 2\alpha_2 S^2 , \quad y_1 = \alpha_2 Y , \quad y_2 = -\alpha_1 + \alpha_2 + \alpha_3 + \alpha_5 , \\
&y_3 = (\kappa-1)\alpha_3 + (\kappa'-1)\alpha_2 - (\kappa+\kappa'-2)\alpha_1 , \quad y_4 = -(\kappa-1)(\kappa'-1)\alpha_1 , \quad t_0 = 3\beta_{10} , \quad t_1 = 6S^2(\beta_3 - \beta_4) , \\
&t_2 = -12S^2\beta_1 , \quad t_3 = 3(\beta_3 Y - \beta_4 Y') , \quad t_4 = -12S^4\beta_1(\kappa+\kappa'-2) , \quad t_5 = -3\beta_1 YY' , \quad t_6 = 3\beta_9 , \\
&t_7 = 3(\beta_5 - \beta_6) + 6S^2(\beta_7 - \beta_8) , \quad t_8 = -3\beta_2 - 12S^2\beta_1 , \quad t_9 = 3[(\kappa-1)\beta_5 - (\kappa'-1)\beta_6 + \beta_7 Y - \beta_8 Y'] , \\
&t_{10} = -3(\kappa+\kappa'-2)(\beta_2 + 4\beta_1 S^2) , \quad t_{11} = -3(\kappa-1)(\kappa'-1)\beta_2 - 3\beta_1[(\kappa-\kappa')^2 + 4(\kappa-1)(\kappa'-1)S^2] .
\end{aligned} \tag{B5}$$

[1]M. Delbrück, note added in proof to L. Meitner and H. Kosters, Z. Phys. 84, 137 (1933).

[2]A review article on Delbrück scattering is being prepared. It will be published in Physics Reports.

[3]R. Karplus and M. Neuman, Phys. Rev. 80, 380 (1950).

[4]F. Rohrlich and R. L. Glückstern, Phys. Rev. 86, 1 (1952).

[5]P. Kessler, J. Phys. Rad. 19, 739 (1958).

[6]W. Zernik, Phys. Rev. 120, 549 (1960).

[7]F. Ehlotzky and G. C. Sheppey, Nuovo Cimento 33, 1185 (1964).

[8]V. Costantini, B. De Tollis, and G. Pistoni, Nuovo Cimento 2A, 733 (1971).

[9]H. Cheng and T. T. Wu, Phys. Rev. 182, 1852 (1969); 182, 1868 (1969); 182, 1873 (1969); 182, 1899 (1969); Phys. Rev. D 5, 3077 (1972).

[10]F. J. Dyson, Phys. Rev. 75, 1736 (1949); see p. 1747.

[11]Paul Papatzacos, thesis, Det Fysiske Seminar i Trondheim No. 5, 1974 (unpublished).

[12]R. Karplus and M. Neuman, Phys. Rev. 83, 776 (1951).

[13]Y. Shima, Phys. Rev. 142, 944 (1966).

[14]G. Basavaraju and P. P. Kane, Nucl. Phys. A149, 49 (1970).

[15]M. Schumacher, F. Smend, and I. Borchert, Nucl. Phys. A206, 531 (1973).

[16]G. Hardie, J. S. DeVries, and C.-K. Chiang, Phys. Rev. C 3, 1287 (1971).

[17]S. Kahane and R. Moreh, Phys. Rev. C 9, 2384 (1974).

[18]H. E. Jackson, G. E. Thomas, and K. J. Wetzel, Phys. Rev. C 9, 1153 (1974).

[19]J. Moffat and M. W. Stringfellow, Proc. R. Soc. A254, 242 (1960).

[20]G. Jarlskog, L. Jönsson, S. Prünster, H. D. Schulz, H. J. Willutzki, and G. G. Winter, Phys. Rev. D 8, 3813 (1973).

[21]H. Bethe and F. Rohrlich, Phys. Rev. 86, 10 (1952).

[22]F. Rohrlich, Phys. Rev. 108, 169 (1957).

[23]I. Øverbø, K. J. Mork, and H. A. Olsen, Phys. Rev. A 8, 668 (1973).